

# Real-Time Pressing Force System for Electrical Connectors on Printed Circuit Boards

Ekkarat Khotabut<sup>1</sup>, Nattawut Tonglim<sup>2</sup> and Chonlatee Photong<sup>1,\*</sup>

<sup>1,\*</sup> Faculty of Engineering, Mahasarakham University, Kham Riang, Kantarawichai, Maha Sarakham, 44150, Thailand

<sup>2</sup> Sony Technology (Thailand) Co., Ltd., 140 Bangkadi Industrial Alley, Bang Kadi, Mueang Pathum Thani District, Pathum Thani, 12000, Thailand

60010352008@msu.ac.th, goko767@gmail.com, and chonlatee.p@msu.ac.th\*

**Abstract.** This paper presents a real-time pressing force display system for the connector pressing machine. The objectives of the research are to analyze the performance of the pressing machine and to ensure that the machine is ready to be used. Traditionally, most manufacturers assign the maintenance workers to measure pressing force using force gauge manually which may cause measurement errors and interrupt the operating processes. This research proposes an alternative system by using the pressure sensor (KEYANCE AP-C33W) to measure the pressure of the front camera connector pressing cylinder of the pressing machine, a microcontroller (Arduino UNO) to receive analogue signals from the pressure sensor and the load cell to measure the pressing force. After that, find the correlation equation of pressing force and analogue value with statistical analysis and then display by the real-time graph of pressing force using the C# program. The experimental results of the proposed system when implemented at the mobile phone manufacturing processes, Sony Technology (Thailand) Co., Ltd., indicated that the pressing force measured from the program has value closed to the pressing force measured by the proposed load cell, while providing the relatively low errors of front camera pressing cylinder, the microphone pressing cylinder and the keypad pressing cylinder of 0.001-0.03 %, 0.001-0.034%, and 0.001-0.015 %, respectively.

part. The packing part is the part that operates about inspecting and packing of the assembled phones from the first part.

From the aforementioned processes, the most important part is the assembling part. This is because of the fact that it is more complicated and more operating processes than the packing part. The process of assembling part consists of 2 sub-parts: phone accessories assembling part and inspecting part. The assembling part operates mainly on the phone accessories assembling on main Printed Circuit Board (PCB) such as a speaker, a keypad, a camera, a signal transmitter, an LCD display and a battery, including external phone part assembling. On the other hand, the inspecting part is the part which inspects both external and internal phone parts such as color checking, phone part quality checking, dent inspecting and etc. The previous survey data pointed out that the most problems occurred were from the phone accessories assembling on main PCB, which may be the damage of connectors during connecting of phone accessories part on the PCB. The most frequently damaged parts of the connectors is the fine pitch board to the board connector in which the phone accessories part connectors such as a front camera, a main camera, an LCD display, a USB port, a battery and a microphone (see Fig.1.).

|             |               |
|-------------|---------------|
| Received by | 16 March 2019 |
| Revised by  | 6 May 2019    |
| Accepted by | 5 June 2019   |

## Keywords:

Pressing force measurement, pressure sensor, load cell, real-time force measurement, electrical connector

## 1. Introduction

There are a number of assembly plants and companies located in Thailand. Sony Technology (Thailand) Co., Ltd. is one of those who produces electronic tools and accessories of mobile phones. Regarding the company, the manufacturing processes consist of two parts; the first part is the assembling part and the second part is the packing

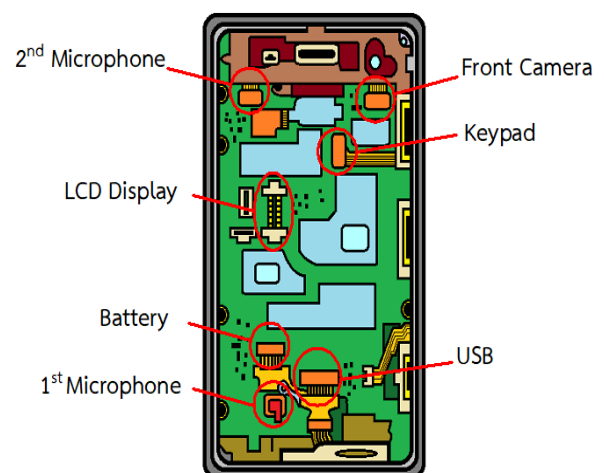


Fig. 1: The parts of phone accessory that need to connect with fine pitch board to board connector [1]

Fig. 2 shows the damage proportions of 6 parts of phone accessory that need to be connected with the fine pitch board to the board connector. From the histogram, the front camera is the highest number of damage over all the other parts (around 0.22 %). Therefore, this research aims to study and reduce the damage of the front camera part connector assembling process.

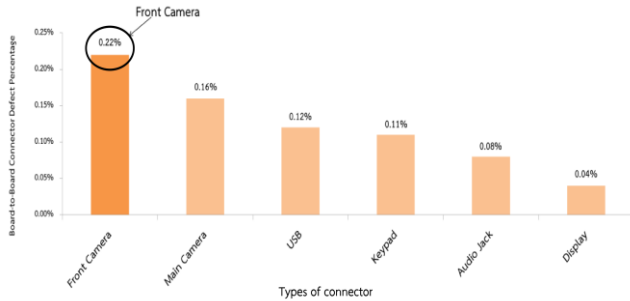


Fig. 2: The percentage of damage occurred from phone accessories part using fine pitch board to board connector [1]

The front camera part assembling process consists of 2 sub-processes. The first sub-process is to determine the position of the connector by the human and the second sub-process is to use the machine to press the same connector to firmly fit to the desired position from the first sub-process again. More details on these sub-processes are as follows:

The first sub-process is for the human operators to manually assemble the connector by observing the golden dashes on the PCB to indicate the mounting position for the connector. When the operators realize that the connecting position is correct, they will use their thumbs to press the connector to fit into the position with suitable pressing force and then use a special tool to press lightly again for setting the connector horizontally. Fig 3 shows the location of golden dashes for pressing the force to fit the connector to the PCB.

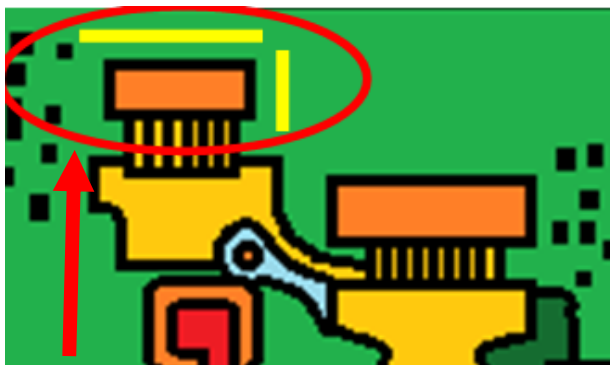


Fig. 3: shows the golden dashes that indicate the position for pressing the connector [1]

Problems of damaging the connector caused by manually pressing could come from many factors. For example, misaligned connecting, unsuitable pressing force,

connector pressing is not horizontally and etc. Those problems affect the connectors or contact surfaces damaged. Fig. 4 shows some examples of misaligned connecting of the connector caused by human operation and Fig. 5 shows an example of the damage on the contact surface that is caused by misaligned connection.

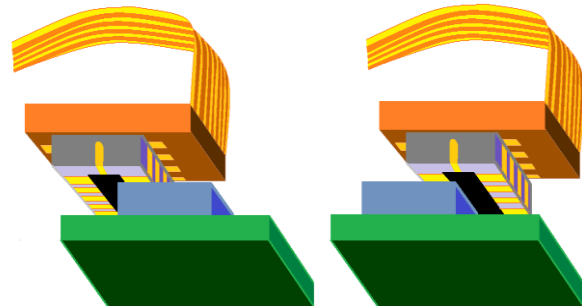


Fig. 4: misaligned connecting of the connector [1]

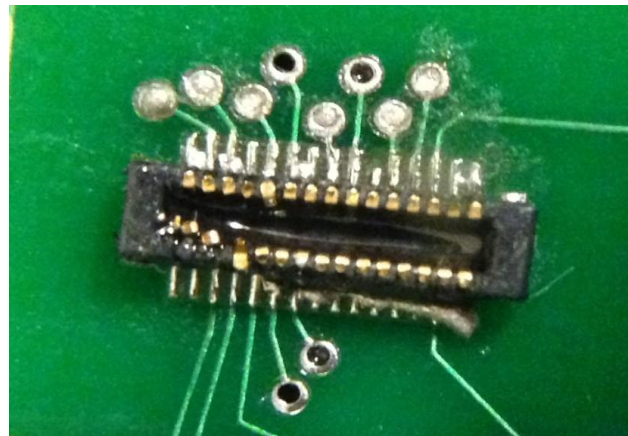


Fig. 5: contact surface of the connector damaged [3]

The second sub-process is the process of the machine that presses the connector to the desired position repeatedly with specified pressing force ( $50 \pm 10\%$  N) at a suitable time ( $3 \pm 1$  s). Unfortunately, as the machine uses air pressure for the pressing operation, and thus is called the pneumatic machine, if the air pressure is not enough, the pressing force of the machine will be low and thus cannot sufficiently press the connectors to the position. On the other hand, if air pressure is higher than the preferred level, the pressing force of the machine will be high and then damage the connectors and sometimes also the main PCB board.

As a result, the researchers propose an alternative method to automatically measure and display the pressing force for the machine so that the machine could always apply suitable pressing force automatically, accurately and efficiently all the times. Some possible solutions would be ones summarized belows:

S.L.Xie, J.P. Mei, H.T. Liu and Y. Wang [4] using the modified Prandtl–Ishlinskii hysteresis feedback control to

control the stroke distance of pneumatic muscle actuator using a distance sensor with pressure sensor and NI PCI-6230 board to receive the analog value from sensors controlled through computer finding, the error of the stroke distance is less than 2 % when compared with the classical Prandtl–Ishlinskii hysteresis feedback control. However, the proposed system relatively has high equipment cost, such as the Data Acquisition (DAQ) card.

M. Sorli and S. Pastorelli [5] simulated force controlling of the servo cylinder using a signal modulation method. This methodology could be applied to any specific actual case of the servosystem.

A.Wache, H.Aschemann, R.Prabel, J.Kurth, B.J.Krause and S.Zorn [6] simulated the control system of the 3-axis pneumatic cylinder of the lung tumor scanner using the cascade feedback control. The proposed control structure has been implemented and validated on a real-time system. The maximum absolute errors for the desired trajectories of the end effector for the y- and z-axes are below 0.3 mm, where the error for the x-axis is approx. 0.5 mm.

P.Yi, R.B.Yuan, W.Long and S.N.Ba [7] using MATLAB to simulate clamping force control system of H-infinity pneumatic robot, the control system can restricts the impact that caused by structure uncertainty and unstructured uncertainty.

C.Ying, Z.J.fan, Y.C.jun and N.Bin [8] proposed the feedback force controlling method of pneumatic robot arms that consists of 2-axis cylinder, high speed on-off valve, DAQ card, fuzzy controller (using Atmega8 microcontroller unit) and using distance sensor and pressure sensor to detect input values. In the experiments, step, slope and sinusoidal commands are taken and the system shows a good performance, and a good agreement is found between the numerical and experimental curves as well.

T.Nakamura and H.Shinohara [9] simulated the force and position control system of the artificial muscle in a pneumatic system that consists of a laser sensor for measuring stretching and contracting distances of the artificial muscle, a pressure sensor, and a force sensor. The control system receives analog data from the sensor, then converts into digital values and finally sends the control signal to proportionally adjust the pressure to be appropriated for the action force.

Research work [10]-[13] provided the theoretical force measuring equipment mentioned that there are 4 common types of force measurement used in the industry, which are detailed as follows:

1. A drawbar force gauge is a force gauge popularly used in lathe working, woodworking, stone cutting and carbon fiber producing. The gauge consists of a strain gauge to get the analog value of pressing force and then convert into a digital signal via an electronic circuit; or else, using a hydraulic pressing cylinder connected with a

pressure gauge for displaying the value of pressing force. However, using the hydraulic gauge may encounter low accuracy because of physical qualification of the gauge display.

2. A dynamometer is a force gauge that used to test work power, horsepower and torque of the engine. It is popularly used in automobile industry.

3. A load cell is a force gauge that measures pressing force or applied weight. The load cell directly converts force or weight into electric signal. Load cell applied to electric weighing machine in industry, tensile strength of material testing, material hardness testing, press fitting testing and etc. But the disadvantage of the load cell is about overloading on the device that can break the cell.

4. A weighting scale is the device used for measuring weight of an object. Weighting scale can be divided by its structure into 2 systems: a mechanical system and an electrical system. The mechanical system utilizes balance leverage, blade mechanism, gears, spring or used multiple systems together for measuring the pressing force or tension force and then change the object weight to monitor display such as needle scale, sliding beam scale, spring scale, dial scale and etc. The electric scale used a load cell to bear the pressing force and display through the LCD. The electrical system is popular for chemical mass measuring and scientific demonstration.

From aforementioned techniques, using of load cell and pressure together and controlling them through a microcontroller is the method used in this paper due to the following reasons,

1. Easy to install and not necessary to adjust structure of the machine by connecting an inlet air tube of connector pressing machine.

2. When using a load cell to measure pressing force that needs to place load cell aligned with pressing cylinder or add an arm part for separating the connector pressing machine and a load cell that helps to support the structure of pressing machine changed.

3. The installation of a pressure sensor can be performed with a pressing cylinder separately and commonly used factor values for considering in the previous pneumatic control system.

4. The microcontrollers have lower price than other controllers or analog converters such as PLC, DAQ card and etc.

According to aforementioned data source, the researcher considers that using of a load cell, a pressure sensor and a microcontroller together, this system could reduce damage of the connector and the circuit board of the mobile phone; and thus consequently helps to provide suitable pressing force of the machine and avoiding affecting damaged product and down time reduced in production process.

## 2. Methodology

This session will discuss about design of the experiment from the collected data, the experimental set-up is worked or not depended on the design process which consists of implementation model, related theories and programming.

### 2.1 Implementation Model

The design of the experiment test-rig consists of 3 parts: implementation on the pressing machine (Forceman), programming and comparison results between the force gauge and the programming.

#### 2.1.1 Pressing Machine (Forceman)

The installation of force measuring device to measure pressing force on the pressing cylinder consists of a pressure sensor connected with an air tube at tip of the cylinder, a load cell joined with force gauge and placed on base of the pressing machine and then place under the pressing cylinder, an air regulator jointed with an air source and a pressure sensor, a multimeter connected with output analog signal of pressure sensor (Fig. 6).

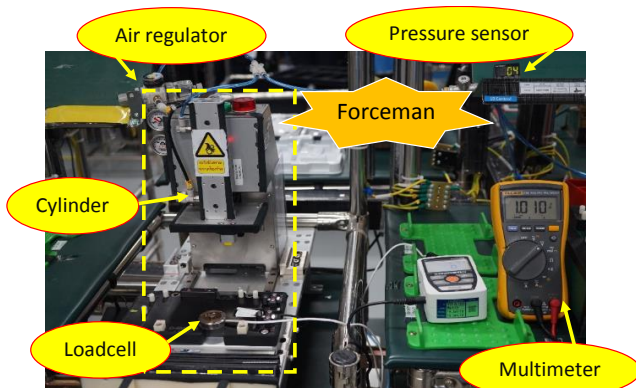


Fig. 6: The overview of force measurement of front camera pressing machine [1]

To measure pressing force of the pressing machine that needs to be used a pressure sensor for measuring air pressure in pressing cylinder and then convert pressure into pressing force via a KEYANCE AP-C33W pressure sensor due to this pressure sensor can detect air pressure from 0 to 1 MPa and the pressure sensor has analog signal pins from 1 to 5 volts. The KEYANCE AP-C33W pressure sensor has 5 wires (as shown in Figs. 7-10), which are specified as follows:

1. The brown wire connected with input 12-24 DC volts
2. The black wire connected with the devices that needs to be controlled (using DC voltage from 5 to 40 volts)

3. The white wire connected with the devices that needs to be controlled (using DC voltage from 5 to 40 volts)
4. The blue wire connected with the ground
5. The pink wire is an output analog signal

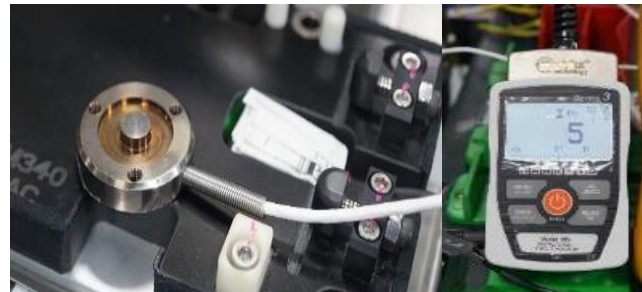


Fig. 7: pressing force measuring equipment of cylinder [1]

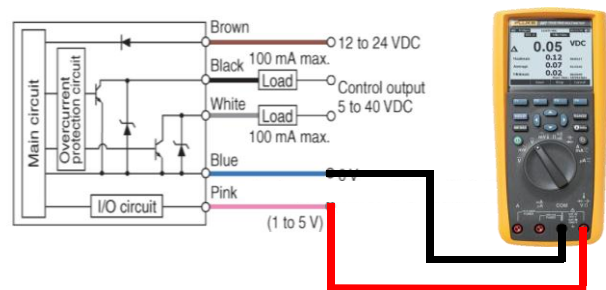


Fig. 8: wiring for measuring analog signal of pressure sensor [1]

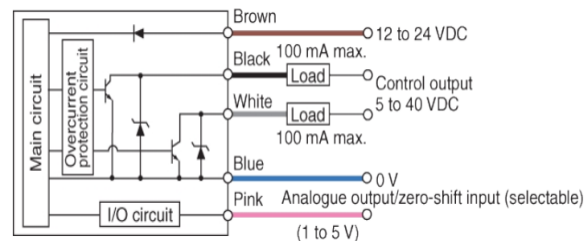


Fig. 9: Internal circuit of AP-C33W pressure sensor [2]

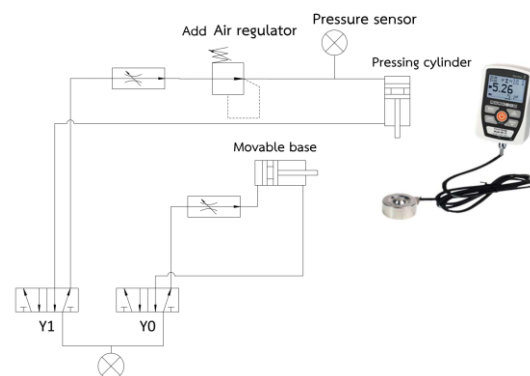


Fig. 10: connecting of force measuring device with Forceman machine [1]

### 2.1.2 Preparing of Experiment

1. Connect the air regulator with the pressing head of the cylinder at the inlet air side.
2. Connect the pressure sensor between the air regulator and the cylinder.
3. Place the load cell aligned with the pressing head of the cylinder.

### 2.1.3 Experimental Procedure

1. Vary the air regulator to increase the air pressure in the cylinder and the inlet pressing force caused by the air pressure with increments of 1 N
2. Press and hold the Y1 solenoid valve for letting the pressing cylinder down on the load cell
3. Measure the air pressure using the pressure sensor in MPa
4. Measure analog voltage of the pressure sensor with the multimeter in volts (V)
5. Measure the force of the pressing cylinder in N
6. Repeat the measurement 1-5 for 3 times
7. Finding the relationship between the air pressure and the pressing force with the regression line

### 2.1.4 Programming principle

The experiment test-rig utilized an Arduino UNO for receiving the analog signal from the pressure sensor through A0 pin on the Arduino board. The connection of the pressure sensor and the Arduino UNO board is depicted in Fig. 11 and the flowchart of programming on the Arduino UNO board is shown in Fig. 12.

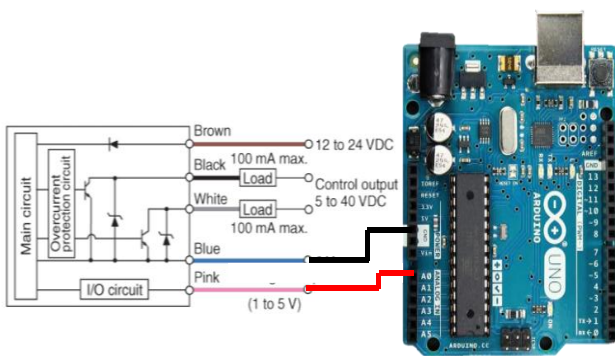


Fig. 11: connecting of pressure sensor and Arduino UNO board

The Arduino is a microcontroller board that sends the data of the pressure sensor to the computer through a serial port with the following principles:

1. The Arduino will send data to the computer when the pressing cylinder presses down on the connector with the pressure higher than 0 MPa or has analog voltage level of 0.197 V (when connected load 1kΩ in parallel).
2. If no pressing or no air pressure inside the pressure sensor, the Arduino will not send the data to the computer and receive the data from the pressure sensor again.

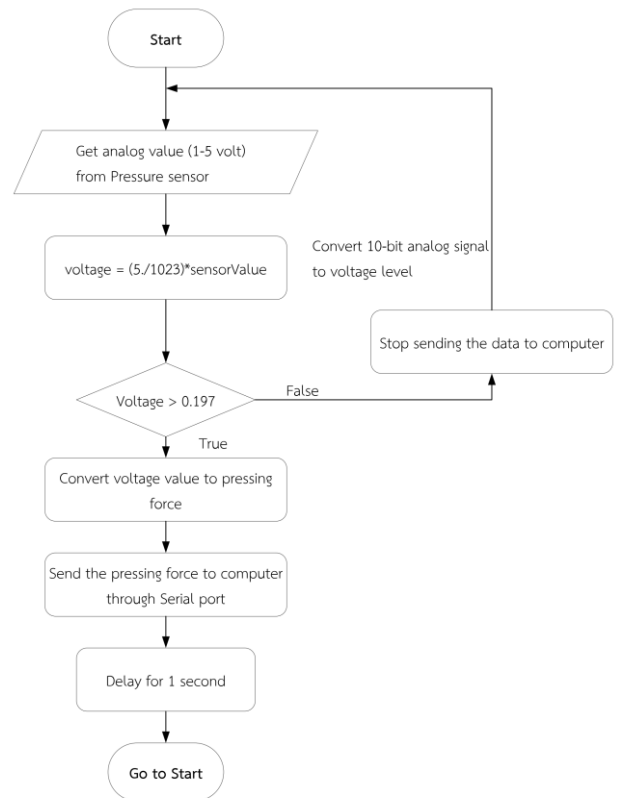


Fig. 12: flowchart of programming on Arduino board

### 2.1.4 Upload Data into Database

The measured data are uploaded into the database by using the AppServ program. The AppServ program is used to simulate via a computer as a server which can be a web server or a database server, then choose the phpMyAdmin for creating a database and then use the python program as a receiver to get the data from the Arduino board for sending data to database as shown in Fig. 13.

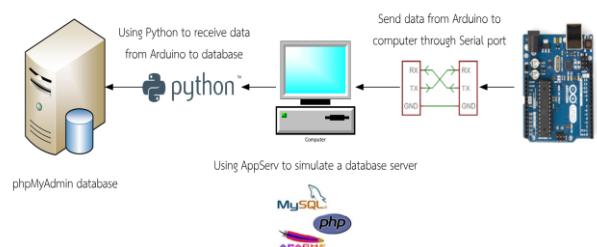


Fig. 13: applying pressing force value from Arduino board and store in database

### 2.1.5 AppServ Program Installation

1. Download the AppServ program from <http://www.appserv.org>
2. Installation the program by following the manual guidance.
3. Rename the server's name as a local host (see Fig. 14), the administrator's email and set the port of the Apache server.



Fig. 14: rename the server's name

4. Set the password for the log in database (Fig. 15)



Fig. 15: set the password for the log in database

5. Press finish button to complete installation (Fig. 16)



Fig. 16: completed the installation

### 2.1.6 Accessing on the phpMyAdmin

1. Log into the web browser

2. Typing the web address with the name "localhost" or the IP address of the computer
3. The web page will show page of the AppServ program as shown in Fig. 17.

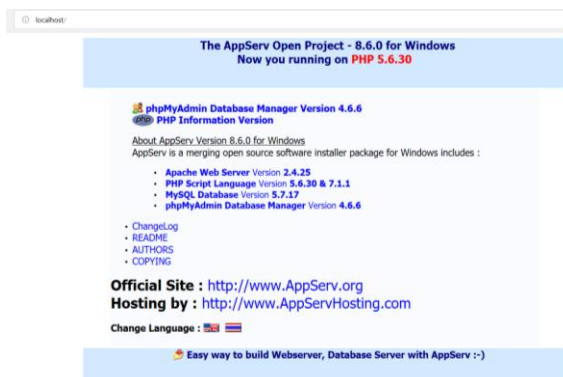


Fig. 17: A page of the AppServ program

4. Access the phpMyAdmin with clicking at "phpMyAdmin Database Manager" link, as shown in Fig. 18.



Fig. 18: Link for accessing phpMyAdmin

5. Log in the database with the username in "root" and name the password as shown in Fig. 19.



Fig. 19: Log in the database

6. Rename the database as “MyDatabase” and then click ‘Create’, as illustrated in Fig. 20.

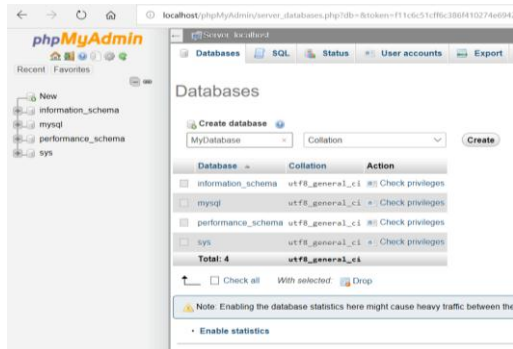


Fig. 20: Rename the database

7. Create the table’s name as “Data” which has 2 columns (first column stores force value and second column stores date, time), see Fig. 21.

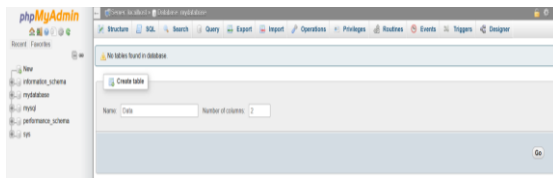


Fig. 21: Create the database table

8. Rename the column’s name (the first column named “ForceData” used to store the pressing force data, the second column named Datetime stores date time) type of data in the ForceData are the decimal format, types of data recorded in Datetime are year/month/day and hour:minute:second format, see Fig. 22.

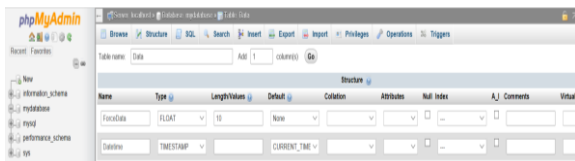


Fig. 22: Rename the column’s name

9. The completed database table (see Fig. 23)

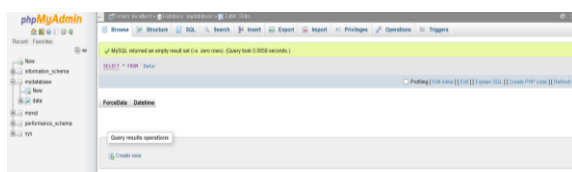


Fig. 23: The completed database table

### 2.1.7 Python Programming

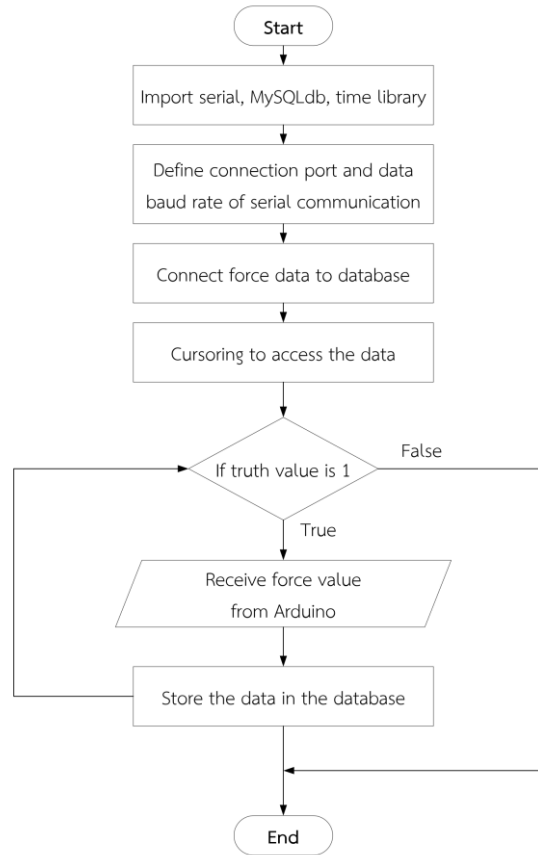


Fig. 24: Diagram shows data sending from microcontroller to database using python programming

## 3. Results

This session presents the experiential results obtained from the proposed system, which have details as follows:

### 3.1 Relationship between pressing force of cylinder and pressure

Record values of 3 variables which are the pressing force of cylinder, the air pressure and the analog voltage of pressure sensor by using measuring tools as follows:

3.1.1 Pressing force of cylinder measured by the Mark-10 M3-012 gauge and a load cell

3.1.2 Air pressure measured by the KEYENCE AP-C33W pressure sensor

3.1.3 The analog voltage of the pressure sensor measured by the FLUKE 117 multimeter

The diagram of the experimental connection shown in Fig. 25 and Fig. 26.

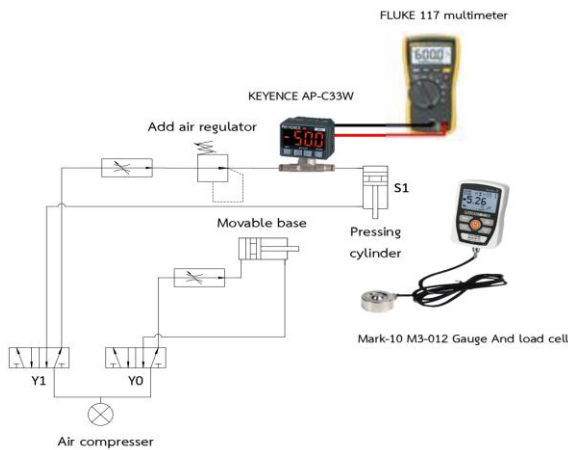


Fig. 25: the details of measuring tools and connecting at the Forceman machine

The first measurement is by varying the pressure from the air regulator by reducing pressure down relatively for decreasing particular pressing force of the cylinder with decrement of 1 N, when pressing force decreased from the previous step as 1 N and then record the pressing force, pressure and voltage of pressure sensor. Record again for 3 times and then synthesize the regression line between the pressing force and pressure, pressing force and analog voltage with the Microsoft Excel.

### 3.2 Comparing between measured pressing force and the pressing force

When obtaining the regression line equation of the pressing force and the measured voltage, then using the equation to calculate in the Arduino UNO board for displaying and storing the pressing force and then choosing the types of cylinder samples as follow: the front camera connector pressing cylinder (SMC MXS8-75 cylinder) microphone connector pressing cylinder (SMC MXS8L-75 cylinder) and the keypad connector pressing cylinder (SMC MXS8-75 cylinder).

The first measurement is by varying the pressure from the air regulator by reducing pressure down gradually for decreasing the pressing force of the cylinder with decrement of 1 N, when the pressing force decreased from previous as 1 N and then recording pressing force from a load cell and the program. Recording again for 3 times and analyzing to determine the regression line between pressing force and pressure, pressing force and analog voltage with Microsoft Excel.

### 3.3 Relationship between pressing force and pressure of cylinder

Table 1 shows the pressing force and the pressure data of the front camera connector pressing cylinder.

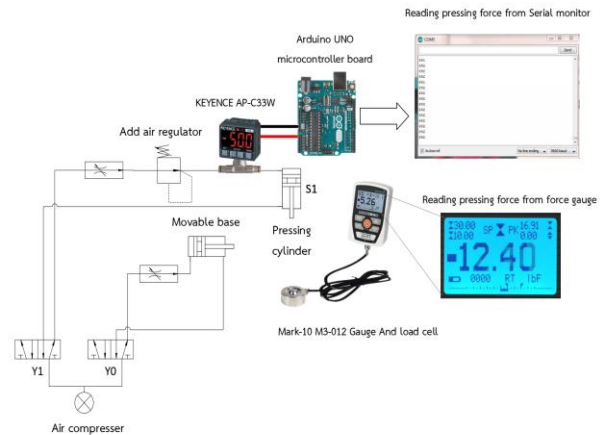


Fig. 26: pressing force that measured by load cell and programming

| Force(N) | Pressure(MPa) |       |       | Average pressure |
|----------|---------------|-------|-------|------------------|
| 20       | 0.199         | 0.196 | 0.189 | 0.195            |
| 21       | 0.206         | 0.205 | 0.204 | 0.205            |
| 22       | 0.216         | 0.214 | 0.214 | 0.215            |
| 23       | 0.228         | 0.229 | 0.226 | 0.228            |
| 24       | 0.235         | 0.236 | 0.233 | 0.235            |
| 25       | 0.242         | 0.247 | 0.242 | 0.244            |
| 26       | 0.259         | 0.257 | 0.254 | 0.257            |
| 27       | 0.264         | 0.263 | 0.266 | 0.264            |
| 28       | 0.276         | 0.278 | 0.273 | 0.276            |
| 29       | 0.283         | 0.292 | 0.282 | 0.286            |
| 30       | 0.299         | 0.300 | 0.300 | 0.300            |
| 31       | 0.305         | 0.309 | 0.305 | 0.306            |
| 32       | 0.315         | 0.318 | 0.314 | 0.316            |
| 33       | 0.326         | 0.328 | 0.335 | 0.330            |
| 34       | 0.333         | 0.344 | 0.344 | 0.340            |
| 35       | 0.343         | 0.354 | 0.352 | 0.350            |
| 36       | 0.357         | 0.361 | 0.366 | 0.361            |
| 37       | 0.364         | 0.372 | 0.374 | 0.370            |
| 38       | 0.377         | 0.381 | 0.383 | 0.380            |
| 39       | 0.392         | 0.398 | 0.398 | 0.396            |
| 40       | 0.400         | 0.403 | 0.405 | 0.403            |
| 41       | 0.409         | 0.411 | 0.413 | 0.411            |
| 42       | 0.414         | 0.424 | 0.426 | 0.421            |
| 43       | 0.424         | 0.431 | 0.434 | 0.430            |
| 44       | 0.440         | 0.444 | 0.441 | 0.442            |
| 45       | 0.453         | 0.448 | 0.453 | 0.451            |
| 46       | 0.458         | 0.465 | 0.464 | 0.462            |
| 47       | 0.470         | 0.471 | 0.478 | 0.473            |
| 48       | 0.484         | 0.486 | 0.484 | 0.485            |
| 49       | 0.487         | 0.493 | 0.489 | 0.490            |
| 50       | 0.497         | 0.498 | 0.499 | 0.498            |

Table 1: Pressing force and pressure data of front camera connector pressing cylinder

### 3.4 Relationship between pressing force and pressure of cylinder

Fig. 27 shows the curves between the pressing force and the pressure of the cylinder according to Table 1.

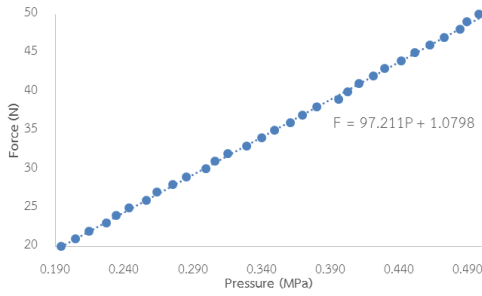


Fig. 27: relationship between pressing force and pressure of cylinder

### 3.5 Relationship between pressing force and voltage that measured by load cell

Measuring of the analog voltage of the pressure sensor by connecting resistor 1kΩ crossed between analog signal and ground wire in Fig. 28. The results shown in Table 2 and Fig. 29.

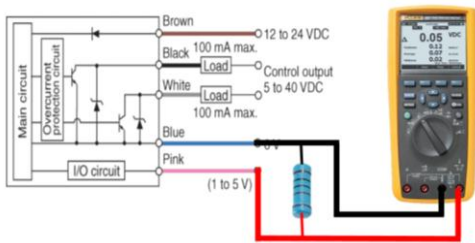


Fig. 28: measurement of analog voltage of the pressure sensor

| Force(N) | Voltage (V) |       |       | Average voltage (V) |
|----------|-------------|-------|-------|---------------------|
| 20       | 0.339       | 0.342 | 0.338 | 0.340               |
| 21       | 0.347       | 0.35  | 0.344 | 0.347               |
| 22       | 0.357       | 0.355 | 0.354 | 0.355               |
| 23       | 0.369       | 0.367 | 0.364 | 0.367               |
| 24       | 0.376       | 0.371 | 0.372 | 0.373               |
| 25       | 0.384       | 0.382 | 0.38  | 0.382               |
| 26       | 0.391       | 0.389 | 0.388 | 0.389               |
| 27       | 0.396       | 0.399 | 0.395 | 0.397               |
| 28       | 0.404       | 0.403 | 0.402 | 0.403               |
| 29       | 0.411       | 0.415 | 0.414 | 0.413               |
| 30       | 0.422       | 0.424 | 0.423 | 0.423               |
| 31       | 0.426       | 0.427 | 0.429 | 0.427               |
| 32       | 0.437       | 0.433 | 0.436 | 0.435               |
| 33       | 0.442       | 0.443 | 0.445 | 0.443               |
| 34       | 0.451       | 0.449 | 0.452 | 0.451               |
| 35       | 0.457       | 0.461 | 0.461 | 0.460               |
| 36       | 0.461       | 0.465 | 0.468 | 0.465               |
| 37       | 0.471       | 0.474 | 0.475 | 0.473               |
| 38       | 0.479       | 0.484 | 0.48  | 0.481               |
| 39       | 0.487       | 0.49  | 0.488 | 0.488               |
| 40       | 0.494       | 0.501 | 0.496 | 0.497               |
| 41       | 0.501       | 0.508 | 0.504 | 0.504               |
| 42       | 0.511       | 0.513 | 0.507 | 0.510               |
| 43       | 0.521       | 0.523 | 0.518 | 0.521               |
| 44       | 0.526       | 0.529 | 0.525 | 0.527               |
| 45       | 0.53        | 0.533 | 0.532 | 0.532               |
| 46       | 0.541       | 0.543 | 0.54  | 0.541               |
| 47       | 0.549       | 0.551 | 0.55  | 0.550               |
| 48       | 0.553       | 0.558 | 0.556 | 0.556               |
| 49       | 0.565       | 0.564 | 0.564 | 0.564               |
| 50       | 0.573       | 0.574 | 0.574 | 0.574               |

Table 2: Relationship between pressing force and voltage data of pressure sensor

### 3.6 Relationship between pressing force and voltage

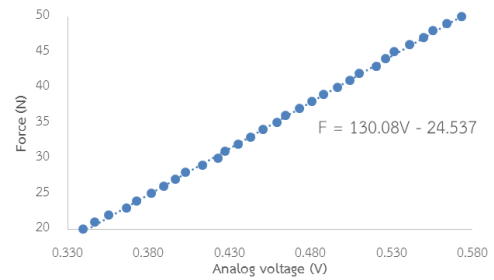


Fig. 29: relationship between pressing force and voltage

The obtained regression line equation of pressing force and analog signal voltage shows the pressing force and the measured voltage from pressure sensor has linear relationship. Therefore, the researcher will use this equation to program in microcontroller; where *Force* is the pressing force (N) and *voltage* is analog signal voltage measured by the pressure sensor (V)

$$Force = 130.08 \times voltage - 24.537 \quad (3.1)$$

### 3.7 Comparison results of measured pressing force from load cell and programming

| Force(N) | Force from Arduino (N) |       |       | Average force(N) | %error |
|----------|------------------------|-------|-------|------------------|--------|
| 20       | 19.97                  | 19.97 | 20.60 | 20.18            | 0.009  |
| 21       | 20.60                  | 21.24 | 20.60 | 20.81            | 0.009  |
| 22       | 21.87                  | 21.87 | 22.51 | 22.08            | 0.004  |
| 23       | 23.15                  | 23.78 | 23.15 | 23.36            | 0.016  |
| 24       | 24.42                  | 24.42 | 23.78 | 24.21            | 0.009  |
| 25       | 25.05                  | 25.05 | 25.69 | 25.26            | 0.011  |
| 26       | 25.69                  | 25.69 | 26.33 | 25.90            | 0.004  |
| 27       | 26.96                  | 26.96 | 27.60 | 27.17            | 0.006  |
| 28       | 27.60                  | 27.60 | 28.23 | 27.81            | 0.007  |
| 29       | 28.87                  | 28.87 | 28.87 | 28.87            | 0.004  |
| 30       | 29.50                  | 30.14 | 30.14 | 29.93            | 0.002  |
| 31       | 30.78                  | 30.78 | 31.41 | 30.99            | 0.000  |
| 32       | 32.05                  | 32.68 | 32.05 | 32.26            | 0.008  |
| 33       | 32.68                  | 33.32 | 33.32 | 33.11            | 0.003  |
| 34       | 33.95                  | 33.95 | 34.59 | 34.16            | 0.005  |
| 35       | 34.59                  | 35.23 | 35.23 | 35.02            | 0.000  |
| 36       | 35.86                  | 35.23 | 36.50 | 35.86            | 0.004  |
| 37       | 37.13                  | 37.13 | 37.77 | 37.34            | 0.009  |
| 38       | 37.77                  | 37.77 | 38.40 | 37.98            | 0.001  |
| 39       | 39.04                  | 39.04 | 39.68 | 39.25            | 0.006  |
| 40       | 39.68                  | 40.31 | 40.31 | 40.10            | 0.003  |
| 41       | 40.95                  | 40.95 | 41.58 | 41.16            | 0.004  |
| 42       | 41.58                  | 41.58 | 42.22 | 41.79            | 0.005  |
| 43       | 42.86                  | 42.86 | 43.49 | 43.07            | 0.002  |
| 44       | 43.49                  | 44.13 | 44.13 | 43.92            | 0.002  |
| 45       | 45.40                  | 46.03 | 45.40 | 45.61            | 0.014  |
| 46       | 46.03                  | 46.03 | 46.67 | 46.24            | 0.005  |
| 47       | 47.31                  | 46.67 | 47.31 | 47.10            | 0.002  |
| 48       | 47.94                  | 47.94 | 47.31 | 47.73            | 0.006  |
| 49       | 48.58                  | 49.21 | 48.58 | 48.79            | 0.004  |

Table 3: front camera connector pressing cylinder (SMC MXS8-75)

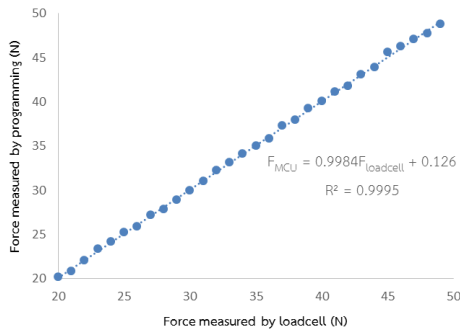


Fig. 30: pressing force that measured from load cell and programming of front camera connector pressing cylinder

| Force(N) | Force from Arduino (N) |       |       | Average force(N) | %error |
|----------|------------------------|-------|-------|------------------|--------|
| 20.00    | 19.33                  | 19.33 | 19.33 | 19.33            | 0.034  |
| 21.00    | 20.60                  | 20.60 | 19.97 | 20.39            | 0.029  |
| 22.00    | 21.87                  | 21.87 | 21.87 | 21.87            | 0.006  |
| 23.00    | 22.51                  | 23.15 | 22.51 | 22.72            | 0.012  |
| 24.00    | 23.78                  | 23.78 | 23.78 | 23.78            | 0.009  |
| 25.00    | 24.42                  | 24.42 | 24.42 | 24.42            | 0.023  |
| 26.00    | 25.05                  | 25.05 | 25.69 | 25.26            | 0.028  |
| 27.00    | 26.96                  | 26.96 | 26.96 | 26.96            | 0.001  |
| 28.00    | 27.60                  | 28.23 | 28.23 | 28.02            | 0.001  |
| 29.00    | 28.87                  | 29.50 | 28.87 | 29.08            | 0.003  |
| 30.00    | 30.14                  | 30.78 | 29.50 | 30.14            | 0.005  |
| 31.00    | 30.78                  | 31.41 | 31.41 | 31.20            | 0.006  |
| 32.00    | 32.05                  | 32.68 | 33.32 | 32.68            | 0.021  |
| 33.00    | 33.32                  | 32.68 | 33.32 | 33.11            | 0.003  |
| 34.00    | 33.95                  | 33.95 | 34.59 | 34.16            | 0.005  |
| 35.00    | 34.59                  | 34.59 | 35.23 | 34.80            | 0.006  |

Table 4: microphone connector pressing cylinder (MXS8L-75)

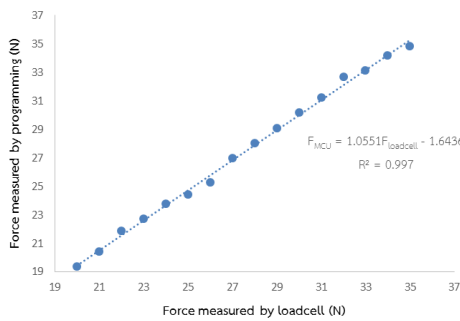


Fig. 31: pressing force that measured from load cell and programming of microphone connector pressing cylinder

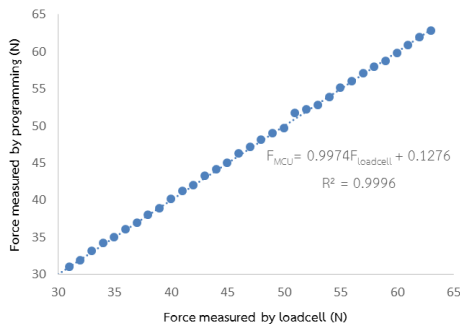


Fig. 32: pressing force that measured from load cell and programming of keypad connector pressing cylinder

| Force(N) | Force from Arduino (N) |       |       | Average force(N) | %error |
|----------|------------------------|-------|-------|------------------|--------|
| 30       | 29.50                  | 30.14 | 29.50 | 29.71            | 0.010  |
| 31       | 30.78                  | 31.41 | 30.78 | 30.99            | 0.000  |
| 32       | 31.41                  | 32.05 | 32.05 | 31.84            | 0.005  |
| 33       | 32.68                  | 33.32 | 33.32 | 33.11            | 0.003  |
| 34       | 33.95                  | 34.59 | 33.95 | 34.16            | 0.005  |
| 35       | 35.23                  | 34.59 | 35.23 | 35.02            | 0.000  |
| 36       | 35.86                  | 36.50 | 35.86 | 36.07            | 0.002  |
| 37       | 37.13                  | 36.50 | 37.13 | 36.92            | 0.002  |
| 38       | 37.77                  | 38.40 | 37.77 | 37.98            | 0.001  |
| 39       | 39.04                  | 38.40 | 39.04 | 38.83            | 0.004  |
| 40       | 39.68                  | 40.31 | 40.31 | 40.10            | 0.003  |
| 41       | 40.95                  | 40.95 | 41.58 | 41.16            | 0.004  |
| 42       | 41.58                  | 42.22 | 42.22 | 42.01            | 0.000  |
| 43       | 43.49                  | 43.49 | 42.86 | 43.28            | 0.007  |
| 44       | 44.13                  | 44.13 | 44.13 | 44.13            | 0.003  |
| 45       | 44.76                  | 44.76 | 45.43 | 44.98            | 0.000  |
| 46       | 46.03                  | 46.03 | 46.67 | 46.24            | 0.005  |
| 47       | 46.67                  | 47.31 | 47.31 | 47.10            | 0.002  |
| 48       | 47.94                  | 47.94 | 48.58 | 48.15            | 0.003  |
| 49       | 49.21                  | 48.58 | 49.21 | 49.00            | 0.000  |
| 50       | 49.85                  | 49.21 | 49.85 | 49.64            | 0.007  |
| 51       | 51.12                  | 51.76 | 52.39 | 51.76            | 0.015  |
| 52       | 52.39                  | 51.76 | 52.39 | 52.18            | 0.003  |
| 53       | 53.03                  | 53.03 | 52.39 | 52.82            | 0.003  |
| 54       | 53.66                  | 53.66 | 54.30 | 53.87            | 0.002  |
| 55       | 54.94                  | 55.57 | 54.94 | 55.15            | 0.003  |
| 56       | 55.57                  | 56.21 | 56.21 | 56.00            | 0.000  |
| 57       | 56.84                  | 57.48 | 56.84 | 57.05            | 0.001  |
| 58       | 58.11                  | 58.11 | 57.48 | 57.90            | 0.002  |
| 59       | 58.75                  | 58.75 | 58.75 | 58.75            | 0.004  |
| 60       | 60.02                  | 59.39 | 60.02 | 59.81            | 0.003  |
| 61       | 60.66                  | 61.29 | 60.66 | 60.87            | 0.002  |
| 62       | 61.93                  | 61.93 | 61.93 | 61.93            | 0.001  |
| 63       | 62.56                  | 63.20 | 62.56 | 62.77            | 0.004  |

Table 5: keypad connector pressing cylinder (MXS8-75)

### 3.8 Comparison results of measured pressing force from load cell and programming of 3 types of cylinders

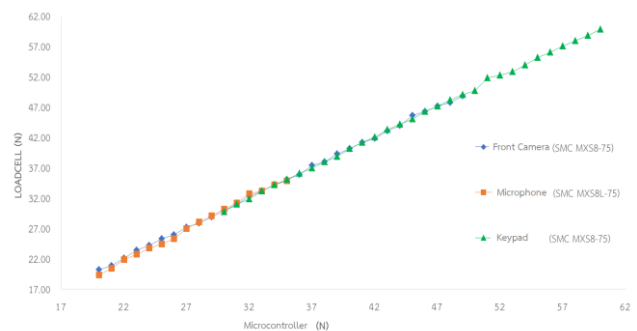


Fig. 33: comparison result of pressing force that measured from load cell and programming of 3 types of cylinder

It can be seen that the results from Fig. 3.8 and Fig. 3.9 are similar. Therefore, concluding that the equation in microcontroller programming can measure the pressing force of the cylinder that has a same length of bore and stroke.

## 4. Conclusions

From the various procedures of applying the equipment in company to design a measuring tool for testing and analyzing the experimental result with find the relationship between pressing force, pressure and voltage from sensor and then program in microcontroller for storing pressing force data, concluded that:

1. The pressing force measured by program are closed to the pressing force measured by load cell and relative error of front camera pressing cylinder is 0.001-0.03 %.

2. The pressing force measured by program are closed to the pressing force measured by the load cell and the relative error of front microphone pressing cylinder is 0.001-0.034 %.

3. The pressing force measured by program are closed the pressing force measured by a load cell and the relative error of keypad pressing cylinder is 0.001-0.015 %.

4. The created measuring tool and the system can measure and store pressing force to the database.

5. The created measuring tool and the system can measure pressing cylinder showed a same length of bore and stroke.

## Acknowledgements

The authors would like to express the great gratitude to Asst. Prof. Niwat Angkawisittpan, Assoc. Prof. Worawat Sa-ngiamvibool, Asst. Prof. Nattawoot Suwannata and all other people who involved in this project for their support, as well as, the Sony Technology (Thailand) Co. Ltd. for the financial support and experiment equipment test-rigs. Finally, the authors would like to thank the Work-integrated Learning (WiL) project for all their support throughout the period of this research.

## References

- [1] Sony Device Technology (Thailand) Co. Ltd.
- [2] [online]. Available: <https://www.keyence.co.th> (Accessed on 17 July 2018)
- [3] [online]. Available: <https://lh3.googleusercontent.com/> (Accessed on 17 July 2018)
- [4] Xie, Shenglong, et al. *Hysteresis modeling and trajectory tracking control of the pneumatic muscle actuator using modified Prandtl-Ishlinskii model*. Mechanism and Machine Theory, 120, 2018, pp. 213-224.
- [5] Sorli, Massimo, and Stefano Pastorelli. *Performance of a pneumatic force controlling servo system: influence of valves conductance*. Robotics and Autonomous Systems, 30.3, 2000, pp. 283-300.
- [6] Wache, Alexander, et al. *Iterative Learning Control of a Pneumatically Actuated Lung Tumour Mimic Model*. IFAC-PapersOnLine, 50.1, 2017, pp. 7,592-7,597.

- [7] Yi, P., et al., *Research for the clamping force control of pneumatic manipulator based on the mixed sensitivity method*. Procedia Engineering, 2012, 31, pp. 1225-1233.
- [8] Ying, Chen, et al. *Design and hybrid control of the pneumatic force-feedback systems for Arm-Exoskeleton by using on/off valve*. Mechatronics, 17.6, 2007, pp. 325-335.
- [9] Nakamura, Taro, and Hitomi Shinohara. *Position and force control based on mathematical models of pneumatic artificial muscles reinforced by straight glass fibers*. Robotics and Automation, 2007 IEEE International Conference on. IEEE, 2007.
- [10] [online]. Available: <https://en.wikipedia.org/> (Accessed on 17 July 2018)
- [11] [online]. Available: <http://dynodynamicsthailand.blogspot.com/> (Accessed on 17 July 2018)
- [12] [online]. Available: <https://www.factomart.com> (Accessed on 17 July 2018)
- [13] [online]. Available from <<http://www.ราชภัฏจตุสดมภ์.net> (Accessed on 17 July 2018)

## Biography



**Ekkarat Khotabut** was born in 1993 at Mahasarakham, Thailand. He graduated with bachelor degree of Electrical Engineering from Mahasarakham University in 2016 and expects to complete a master degree of Electrical and Computer Engineering from the same university in 2019 under the scholarship of Work-integrated learning (WIL) project.



**Nattawut Tonglim** graduated from Rajamangala University of Technology Suvarnabhumi, Thailand. He is currently working at Sony Technology (Thailand) Co. Ltd., Thailand.



**Chonlatee Photong** received his B.Eng. from Khon Kaen University, Thailand in 2001. He has been worked at Sony Device Technology (Thailand) Co., Ltd. and Seagate Technology (Thailand) Co., Ltd. for 3 and 2 years, respectively, after that. He received his M.Sc in Power Electronics and Drives and Ph.D. in Electrical and Electronic Engineering from University of Nottingham, UK, in 2013. He is currently the bachelor program director of Practical Engineering (Continuing Program) and a lecturer in Power Electronics and Drives at the Faculty of Engineering, Mahasarakham University, Thailand. His research interests include power electronics, power converters for renewable energy conversion, and electrical machines and drives.